



Full paper/Mémoire

## Alkaline earth metal (II) complexes of vitamin B13 with bidentate orotate ligands: Synthesis, structural and thermal studies

Moamen S. Refat <sup>a,\*</sup>, Samir Alghool <sup>a</sup>, Hanan F. Abdel El-Halim <sup>c</sup><sup>a</sup> Department of Chemistry, Faculty of Science, Port Said University, Port Said, Egypt<sup>b</sup> Department of Chemistry, Faculty of Science, Taif University 888, Taif, Saudi Arabia<sup>c</sup> Department of pharmaceutical Chemistry, Faculty of pharmacy, Misr International University, Cairo, Egypt

## ARTICLE INFO

## Article history:

Received 17 December 2009

Accepted after revision 26 April 2010

Available online 15 September 2010

## Keywords:

Orotic

Alkaline earth

Complexes

Kinetic thermodynamic parameters

Bacterial

## ABSTRACT

Alkaline earth metal Ca(II), Mg(II), Ba(II) and Sr(II) were synthesized by reaction of metal(II) chlorides with orotic acid by molar ratio 1:2 metal-to-ligand. All metal complexes were characterized by different physicochemical methods, elemental analysis, molar conductivity, (Infrared and <sup>1</sup>H-NMR spectra) and simultaneous thermal analysis (TG and DTG) techniques. It has been found from the elemental analysis as well as thermal studies that the orotate complexes behave as bidentate ligand by N1-H and O of carboxylic group, forming chelates with 1:2 (metal: ligand) stoichiometry for all complexes. The molar conductivity measurements proved that the complexes are non-electrolytes. The kinetic thermodynamic parameters such as:  $\Delta E^\ddagger$ ,  $\Delta H^\ddagger$ ,  $\Delta S^\ddagger$  and  $\Delta G^\ddagger$  are calculated from the DTG curves. The entropy of the activation was found to have negative values in all of the complexes. The antibacterial activity of the orotate complexes was evaluated against some kind of gram positive and Gram negative bacteria.

© 2010 Académie des sciences. Published by Elsevier Masson SAS. All rights reserved.

### 1. Introduction

Orotic acid (Vitamin B<sub>13</sub>) and its salts play an important role in biological systems as precursors of the pyrimidine nucleotide and are found in cells and body fluids of many living organisms; these compounds are applied in medicine as biostimulators of the ionic exchange processes in organisms. There is also a great interest for orotic acid in relation to food protection and nourishment research [1–3]. The coordination chemistry of orotic acid continues to attract attention, research in this area ranging from bioinorganic [4] to medicinal [5–7] and materials chemistry [8–10]. It has been established that during these processes the presence of metal ions, especially Mg<sup>2+</sup>, is necessary, particularly during the phosphoribosylation of orotic acid [11]. Metal orotates are widely applied in medicine [12]. Platinum, palladium and nickel orotate

complexes have been screened as therapeutic agents for cancer [13].

The orotic acid molecule (H<sub>2</sub>L) has a multidentate nature (Fig. 1). The most potential coordination sites in the pH range of (pH = 5–9) are the carboxylic oxygen and the adjacent pyrimidine nitrogen atom (N1), for the formation of a stable chelate ring. In very alkaline solutions, deprotonation occurs from (N1) and coordination through the other sites becomes available as well due to the existence of different tautomeric forms [14–16]. UV light absorption studies, potentiometry and linear free energy relationships for proton dissociation [17] have been used to investigate the complexation of zinc(II), cobalt(II), manganese(II), cadmium(II), copper(II) and nickel(II) with orotic acid in solution. It was concluded that, in neutral or slightly acidic pH, the ions of Zn(II), Co(II), Mn(II) and Cd(II) coordinate through the carboxylate group while Cu(II) and Ni(II) through the carboxylate and adjacent N(1). Spectroscopic investigation of the interaction of nickel(II) with orotic acid [18] revealed binding of the metal to the carboxylate and, in some cases, to the adjacent N(1) and the

\* Corresponding author.

E-mail address: msrefat@yahoo.com (M.S. Refat).

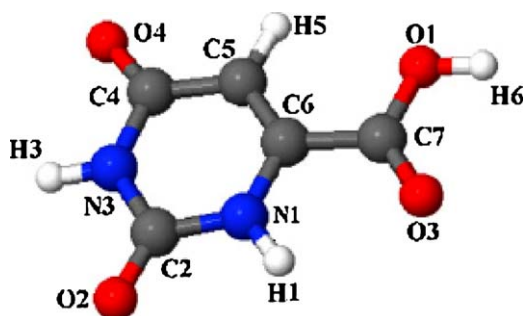


Fig. 1. Structure of orotic acid.

O(4) sites. The crystal structures of the Ni(II) [19,20], Mg(II) [21], Co(II) [22], Zn(II) [23] orotate complexes have been described where orotate dianions act as bidentate ligand.

The complexes of alkaline earth metal cations have recently received an increasing attention in bioorganic chemistry [24]. The coordination behavior of  $Mg^{2+}$  and  $Ca^{2+}$  has attracted the interest of many researches because of the significant role of these ions in biological processes [25–27]. Coordination takes place mainly through ion-dipole and ion-induced dipole interactions, which make dominant contribution to binding. There is, however, a possibility of covalent interaction via delocalization of electron density from occupied ligand orbitals into empty s- or p-orbitals [28]. Here we discuss in this article the synthesis, characterization, thermal and biological activities of alkaline earth metal complexes Ca(II), Mg(II), Ba(II) and Sr(II) of orotic acid.

## 2. Experimental

### 2.1. Materials and instrumentation

All chemicals were reagent grade and were used without further purification. Orotic acid was purchased from Aldrich Chemical Co., and  $MgCl_2$ ,  $SrCl_2$ ,  $CaCl_2$  and  $BaCl_2$  from Fluka. Carbon and hydrogen contents were determined using a Perkin-Elmer CHN 2400 in the Micro-analytical Unit at the Faculty of Science, Cairo University,

Egypt. The metal content was found gravimetrically by converting the compounds into their corresponding oxides. IR spectra were recorded on Bruker FT-IR Spectrophotometer ( $4000\text{--}400\text{ cm}^{-1}$ ) in KBr pellets.  $^1\text{H-NMR}$  spectrometer was recorded using DMSO as solvent, chemical shift are given in ppm relative to tetramethylsilane. Molar conductivities of freshly prepared  $1.0 \times 10^{-3}\text{ mol/dm}^3$  DMSO solutions were measured using Jenway 4010 conductivity meter. Thermogravimetric analysis (TG and DTG) were carried out in dynamic nitrogen atmosphere (30 ml/min) with a heating rate of  $10\text{ }^\circ\text{C/min}$  using a Shimadzu TGA-50H thermal analyzer. The elemental analysis and some physical properties are summarized in Table 1.

### 2.2. Synthesis of the coordination complex

The complexes were synthesized by reactions of metal(II) chlorides and the ammonium salt of orotic acid in aqueous solution, in amounts equal to metal:ligand molar ratio of 1:2. The complexes were prepared by adding an aqueous solution of Ca(II), Sr(II) Ba(II) and Mg(II) salt to an aqueous solution of the ammonium salt of orotic acid. The reaction mixture was stirred with an electromagnetic stirrer at  $40\text{ }^\circ\text{C}$  for 2 h. At the moment of mixing of the solutions, a precipitate was obtained. The precipitate was filtered (pH of the filtrate was 6.5), washed several times with water (20 ml hot water), alcohol (15 ml), and dried in vacuo over  $CaCl_2$  to constant weight. The complexes resulted have low solubility in water and in common organic solvents and well soluble in DMSO. The analytical data are in a good agreement with the proposed stoichiometry of the complexes. All complexes decomposed at temperatures higher than  $250\text{ }^\circ\text{C}$ . Elemental analyses (Table 1) were in good agreement with those required for the purpose of formula.

### 2.3. Antibacterial investigation

For these investigations the filter paper disc method was applied. The investigated isolates of bacteria were seeded in tubes with nutrient broth (NB). The seeded NB ( $1\text{ cm}^3$ ) was homogenized in the tubes with  $9\text{ cm}^3$  of melted ( $45\text{ }^\circ\text{C}$ )

Table 1  
Elemental analyses and physical data of Ca(II), Mg(II), Ba(II) and Sr(II) complexes.

Complexes M.F/M.Wt	Molar Conductance $\Omega^{-1}\text{cm}^2\text{mol}^{-1}$	M.P/ $^\circ\text{C}$	Yield (%)	Elemental analyses			
				%C	%H	%N	%M
$[\text{Ca}(\text{L}_2 \cdot 2\text{H}_2\text{O})] \cdot \text{H}_2\text{O}$ $\text{C}_{10}\text{H}_{10}\text{N}_4\text{O}_{11}\text{Ca}/$ 402 (I)	11	> 300	79	29.68 (29.19)	2.51 (2.66)	13.93 (13.23)	9.96 (10.11)
$[\text{Mg}(\text{L}_2 \cdot 2\text{H}_2\text{O})] \cdot 4\text{H}_2\text{O}$ $\text{C}_{10}\text{H}_{16}\text{N}_4\text{O}_{14}\text{Mg}/$ 440.05 (II)	14	> 300	86	27.26 (26.98)	3.66 (3.82)	12.72 (12.56)	5.52 (5.17)
$[\text{Ba}(\text{L}_2 \cdot 2\text{H}_2\text{O})] \cdot 2\text{H}_2\text{O}$ $\text{C}_{10}\text{H}_{12}\text{N}_4\text{O}_{12}\text{Ba}/$ 517.95 (III)	13	> 300	82	23.21 (23.61)	2.34 (2.61)	10.83 (11.11)	26.53 (25.82)
$[\text{Sr}(\text{L}_2 \cdot 2\text{H}_2\text{O})] \cdot \text{H}_2\text{O}$ $\text{C}_{10}\text{H}_{10}\text{N}_4\text{O}_{11}\text{Sr}/$ 449.94 (IV)	16	> 300	78	26.70 (26.54)	2.24 (2.36)	12.46 (12.28)	19.48 (19.01)

**Table 2**  
Infrared spectra of ligands H<sub>2</sub>L and their Ca(II), Mg(II), Ba(II) and Sr(II) complexes.

H <sub>2</sub> L	I	II	III	IV	Assignments
–	3416(br)	3399(br)	3415(br)	3420(br)	$\nu$ (OH) hydrated
–	3305(br)	3280(br)	3326(br)	3315(br)	$\nu$ (OH) Coord.
1660(s)	1656(s)	1655(s)	1650(s)	1658(s)	$\nu$ (C=O)
3386(br)	–	–	–	–	$\nu$ (OH) (COOH)
1710	1717	1709	1694	1707	$\nu$ (C=O) (COOH)
3066(m)	–	–	–	–	$\nu$ (N <sub>1</sub> –H)
3190(m)	3192(m)	3189(m)	3179(m)	3180(m)	$\nu$ (N <sub>3</sub> –H)
–	543(w)	539(w)	543(w)	547(w)	$\nu$ (M–N)
–	419(w)	431(w)	440(w)	420(w)	$\nu$ (M–O)

nutrient agar (NA). The homogeneous suspensions were poured into Petri dishes. The discs of filter paper (diameter 5 mm) were ranged on the cool medium. After cooling on the solid medium formed,  $2 \times 10^{-5} \text{ dm}^3$  of the investigated compounds were applied using a micropipette. After incubation for 24 h in a thermostat at 25–27 °C, the inhibition (sterile) zone diameters (including disc) were measured and expressed in mm. An inhibition zone diameter over 8 mm indicates that the tested compound is active against the bacteria under investigation. The antibacterial activities of the investigated compounds were tested against *Escherichia coli* and *Salmonella* (Gram negative bacteria) and *Bacillus subtilis* and *Staphylococcus aureus* (Gram positive bacteria). The ligand was also tested, as well as the pure solvent. The concentration of each solution was  $5 \times 10^{-3} \text{ mol dm}^{-3}$ . DMSO was employed to dissolve the tested samples.

### 3. Results and discussion

The selected physical properties and characteristic data of the synthesized metal complexes were measured and listed in (Table 1). The complexes were synthesized using a 1:2 (metal:ligand) mole ratio of all reactants. The complexes are air-stable, hygroscopic, with high melting points. The metal complexes are insoluble in common organic solvents in cold or hot conditions, but are generally soluble in DMSO. The molar conductivities of  $10^{-3} \text{ mol dm}^{-3}$  solutions of the complexes in DMSO (Table 1) indicate that the complexes are non-electrolytes. It is worth mentioning that most studies of orotic acid complexes in the solid phase have found that orotic acid is in the dianion form [29–32]. It is, therefore, of great interest to examine the coordination behavior of orotic acid at neutral pH values. This study were used many techniques of analysis to prove the structure of

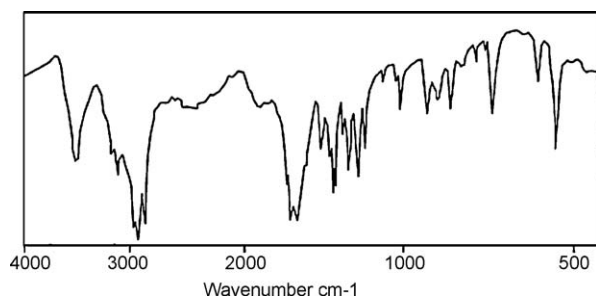


Fig. 2. Infrared spectra of orotic acid.

the synthesized complexes. According to the elemental analyses, IR, UV–vis, and thermogravimetric data, the complexes of the bidentate ligands had two coordinated water molecules.

#### 3.1. IR spectra

The coordination mode of the orotate ligand may be discussed on the basis of the comparison of the IR spectra of the free orotic acid (Table 2 and Fig. 2). The IR spectra of the Ca(II), Mg(II), Sr(II) and Ba(II) complexes exhibited characteristic features (donation sites) in the –OH (acid), ketone (C(2)=O and C(4)=O), carboxylate and NH (N(1)–H and N(3)–H) regions. The IR spectra of the Ca(II), Mg(II), Sr(II) and Ba(II) orotates show characteristic frequencies in the ranges 3100–3200  $\text{cm}^{-1}$  and  $\sim 1430 \text{ cm}^{-1}$  (Table 2 and Fig. 3), which are attributable to NH stretching and deformation, respectively.

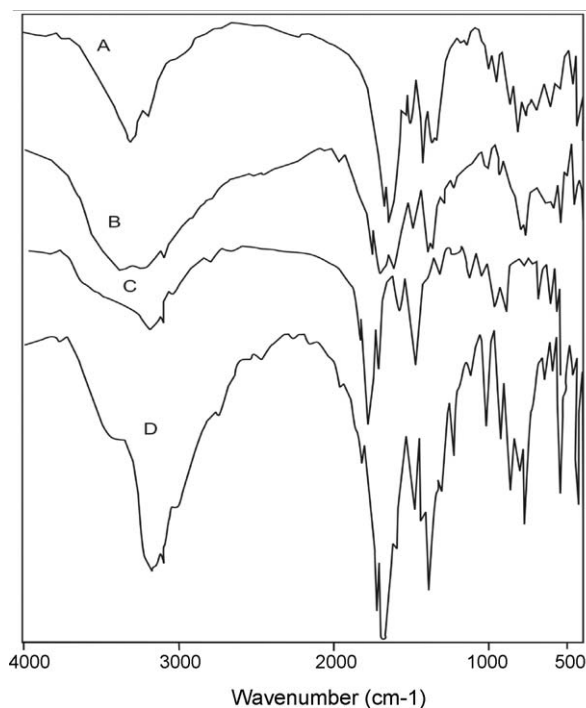


Fig. 3. Infrared Spectra of: A =  $[\text{Ca}(\text{L})_2(\text{H}_2\text{O})_2] \cdot \text{H}_2\text{O}$ ; B =  $[\text{Mg}(\text{L})_2(\text{H}_2\text{O})_2] \cdot 4\text{H}_2\text{O}$ ; C =  $[\text{Ba}(\text{L})_2(\text{H}_2\text{O})_2] \cdot 2\text{H}_2\text{O}$ ; D =  $[\text{Sr}(\text{L})_2(\text{H}_2\text{O})_2] \cdot \text{H}_2\text{O}$ .

Coordination and crystal water stretching modes appear between 3420–3280  $\text{cm}^{-1}$  with the crystal water appearing at frequencies higher than these of coordination product [33]. The deprotonation of N(1) confirmed from the disappearance of the bands at *ca.* 3100 and 1430  $\text{cm}^{-1}$  attributed to the stretching and bending N(1)–H vibrations. This is noted in cases where the orotate bind through the N(1) atom is shifted and observed within the  $\sim 1715$  and  $\sim 1300$   $\text{cm}^{-1}$  bands, corresponding to the asymmetric and symmetric stretching of the carboxylate group which appear at  $\sim 1690$  and  $\sim 1370$   $\text{cm}^{-1}$ . These shifts are expected, indicating an interaction between the metal and the carboxylate group. Deprotonation of OH of carboxylate group results in disappearance of the bands at *Ca.* 3500. The presence of water molecules perhaps outside or inside coordination sphere of the complexes, also the presence of strong band at  $\sim 850$   $\text{cm}^{-1}$  in all complexes attributed to the rocking vibration motion,  $\nu(\text{H}_2\text{O})$ , of coordination water molecules; this confirms that  $\text{H}_2\text{O}$  molecules in the complexes are inside the coordination sphere. This notification was also supported by thermal analysis. The crystal structure of the  $[\text{Ni}(\text{HOA})(\text{H}_2\text{O})_4]\cdot\text{H}_2\text{O}$  [19] and  $[\text{Cu}(\text{HOA})(\text{NH}_3)_2]$  [34] complexes showed bidentate binding of orotic acid through N(1) and the carboxylate group. In the infrared spectra of the complexes, bands were detected at 539–547  $\text{cm}^{-1}$  and 419–440  $\text{cm}^{-1}$  may be assigned to M–N and M–O, respectively.

### 3.2. $^1\text{H-NMR}$ spectra

The  $^1\text{H-NMR}$  spectral data of the  $[\text{Ca}(\text{L})_2(\text{H}_2\text{O})_2]\cdot\text{H}_2\text{O}$  complex and the free ligand orotic acid [35] are collected in Table 3 and its spectrum is shown in Fig. 4. The  $^1\text{H-NMR}$  chemical shifts (*d*, ppm) of orotic acid are included in Table 3 for comparison purposes. The presence of the N(1)–H and N(3)–H protons resonance in the spectrum (Table 3 and Fig. 4) clearly show that this nitrogen atom engaged (N(1)–H) in the complex formation. The absence of proton of (COOH) confirm the mode of coordination (behaves as a bidentate chelating ligand). The broad singlet peak at 4.35 ppm is due to the presence of water molecules

**Table 3**  
H-NMR data of orotic acid and Ca(II) complex.

Compound	$\text{H}_2\text{O}$ Coord.	N(1)–H	N(3)–H	C(5)–H	OH acid
Orotic acid	–	8.84	9.87	6.38	10.49
$[\text{Ca}(\text{L}_2, 2\text{H}_2\text{O})]\cdot\text{H}_2\text{O}$	4.35	–	9.27	6.32	–

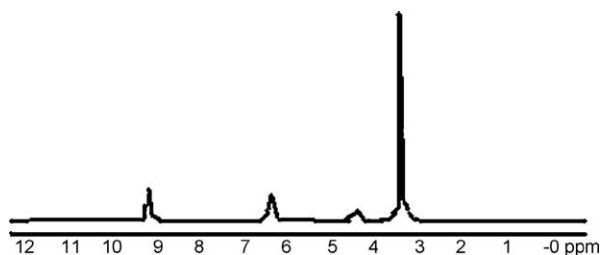
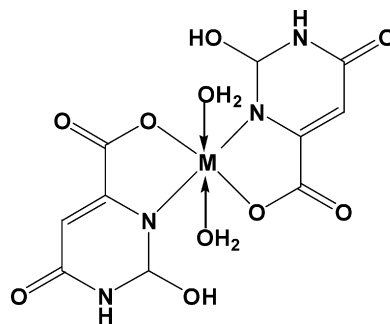


**Fig. 4.** H-NMR Spectra of Ca(II) complex.



**Scheme 1.** The proposed structures of the orotate complexes.

protons and a multiplet signal around 6.32 ppm is due to the (C5)–H aromatic protons.

The proposed structures of the synthesized complexes which are presented in Scheme 1 are consistent with each other in term of chemical and spectroscopic data.

### 3.3. Thermogravimetric analysis

Thermal analysis curves (TG and DTG) of the studied complexes are shown in Fig. 5. The cause of higher temperature for liberated crystallized water molecules is due to the hydrogen bonding interaction with the coordination water molecules and orotate anions. Based on the essential  $\text{DTG}_{\text{max}}$  temperatures of the decomposition of orotate complexes, the thermal interpretation may be designed as follows:

The thermal analysis curves of the Ca(II) complex show that decomposition takes places in three stages in 25–800  $^{\circ}\text{C}$  temperature range (Fig. 5). The first exothermic decomposition stage corresponds to the dehydration process. The DTG and TG curves of the complex show a weight loss (found 4.76, *calcd.* 4.47%) in the 25–150  $^{\circ}\text{C}$  range corresponding to the loss of one molecule of water. The second stage, two coordinated water molecules were lost in between 150–350  $^{\circ}\text{C}$ . The following stage is also exothermic in between 350–600  $^{\circ}\text{C}$ , (DTG) showing the decomposition of orotic acid. The final product, formed at *Ca.* 700  $^{\circ}\text{C}$ , consists of (CaO with contaminated carbon atoms) with (found 17.10%, *calcd.* 16.69%). Sufficient oxygen atoms helped to evolve carbon as carbon monoxide or dioxide.

Thermal decomposition of Mg(II) complex proceeds in four ranged main stages. The hydrated water molecules are associated with complex formation and found outside the coordination sphere formed around the central metal ion. The dehydration of this type of water takes place in the temperature range 25–140  $^{\circ}\text{C}$ . The weight loss corresponds to four water molecules (found 17.00%, *calcd.* 16.36%), the coordinated water molecules are eliminated at higher temperature than the water molecules of hydration. The water of coordination was lost in the temperature range 100–316  $^{\circ}\text{C}$ , corresponding to loss of two coordination water molecules (found 8.64%, *calcd.* 8.18%). The following stage is also exothermic in between 400–650  $^{\circ}\text{C}$ , showing the decomposition of orotic acid. The final decomposition products are MgO with residual carbon (found 8.05%, *calcd.* 9.09%).

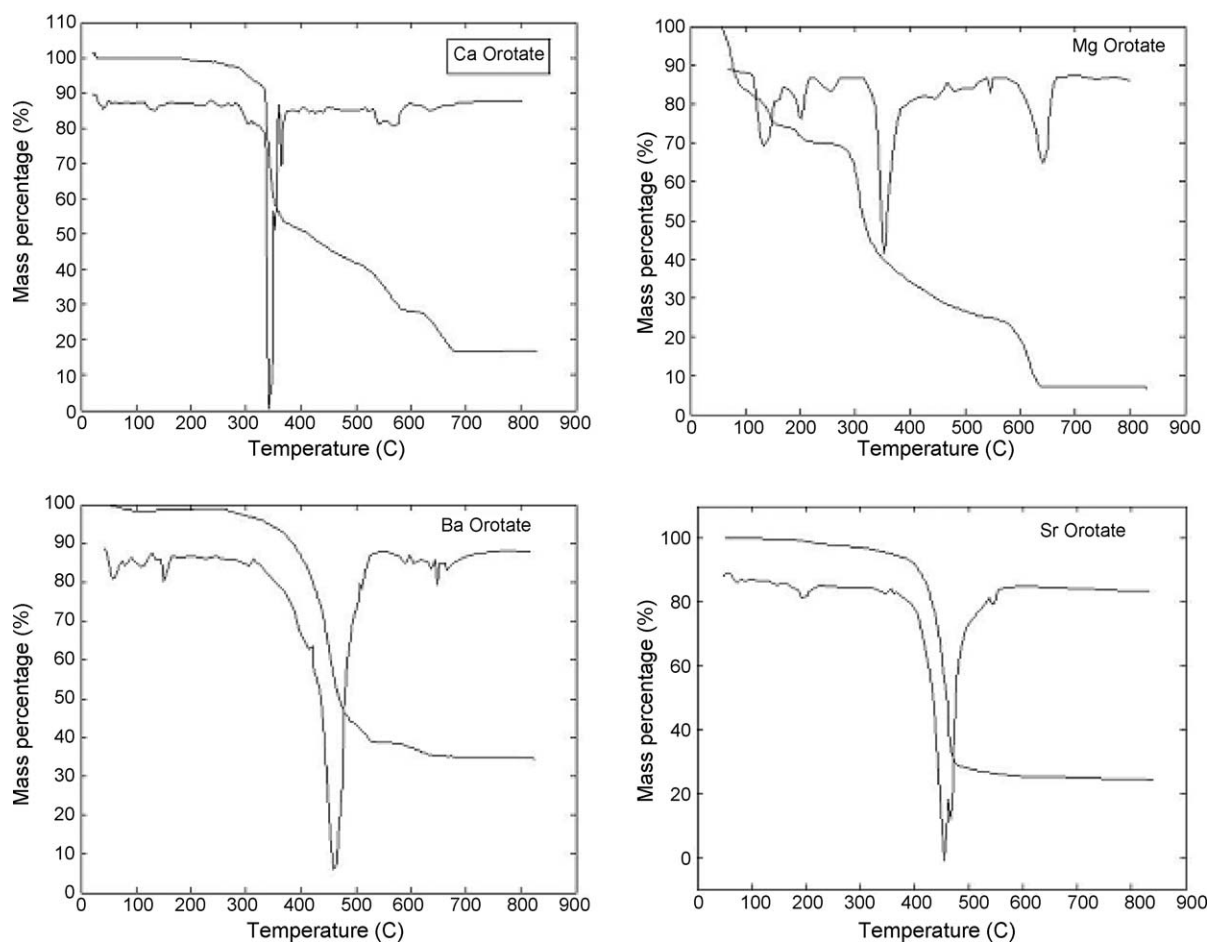


Fig. 5. TGA diagram of Ca(II), Mg(II), Ba(II) and Sr(II) orotate complexes.

Thermal analysis curves of Ba(II) complex show that decomposition take places in three stages in temperature range 25–800 °C. The TG curve of the Ba(II) complex show a weight loss (found 6.43%, calcd. 6.94%) between 25–150 °C corresponding to the loss of two hydration water molecules. The second stage shows a weight loss (found 6.24%, calcd. 6.94%) between 150–350 °C corresponding to the loss of two coordinated water molecules. The final product formed at 750 °C consist of BaO and carbon residual (found 33.78%, calcd. 34.16%).

The diagrams of the Sr(II) complex reveals mass loss in temperature range 30–800 °C; three stages are shown in the pyrolysis curve, the first stage corresponding to the dehydration of one water molecule (found: 3.87%, calcd. 4.00%). The second stage was discussed concerning the loss of two coordinated water molecules, weight loss (found: 7.77%, calcd.: 8.00%). The following stage is in between 350–600 °C, showing the decomposition of orotic acid. The final decomposition product is SrO (found 24.04%, calcd. 23.11%).

#### 3.4. Kinetic studies

Coats–Redfern [36] is the method mentioned in the literature related to kinetic thermodynamic studies; this

method is applied in this study. From the TG curves, the activation energy,  $E$ , pre-exponential factor,  $A$ , entropy,  $\Delta S$ , enthalpy,  $\Delta H$ , and Gibbs free energy,  $\Delta G$ , were calculated by well-known methods; where  $\Delta H = E - RT$  and  $\Delta G = \Delta H - T\Delta S$ . The linearization curves of the Coats–Redfern method is shown in Fig. 6. Kinetic parameters are calculated by employing the Coats–Redfern equations, and are summarized in Table 4. The activation energies of the complexes were found to be in the range 134–208 J mol<sup>-1</sup>. According to the kinetic data obtained from DTG curves, the high values of the activation energies reflect the thermal stability of the complexes. The entropy of the activation was found to have negative values in all of the complexes. Negative values indicate that the reactions proceed with disorder due to the decomposition of the complexes.

#### 3.5. Bactericidal investigations

The biological activity of orotic acid and their metal complexes were tested against bacteria; we used more than one test organism to increase the chance of detecting antibiotic principles in tested materials. The organisms used in the present investigations included two Gram positive bacteria (*B. subtilis* and *S. aureus*) and two Gram negative bacteria (*E. coli* and *Pseudomonas aeruginosa*). The

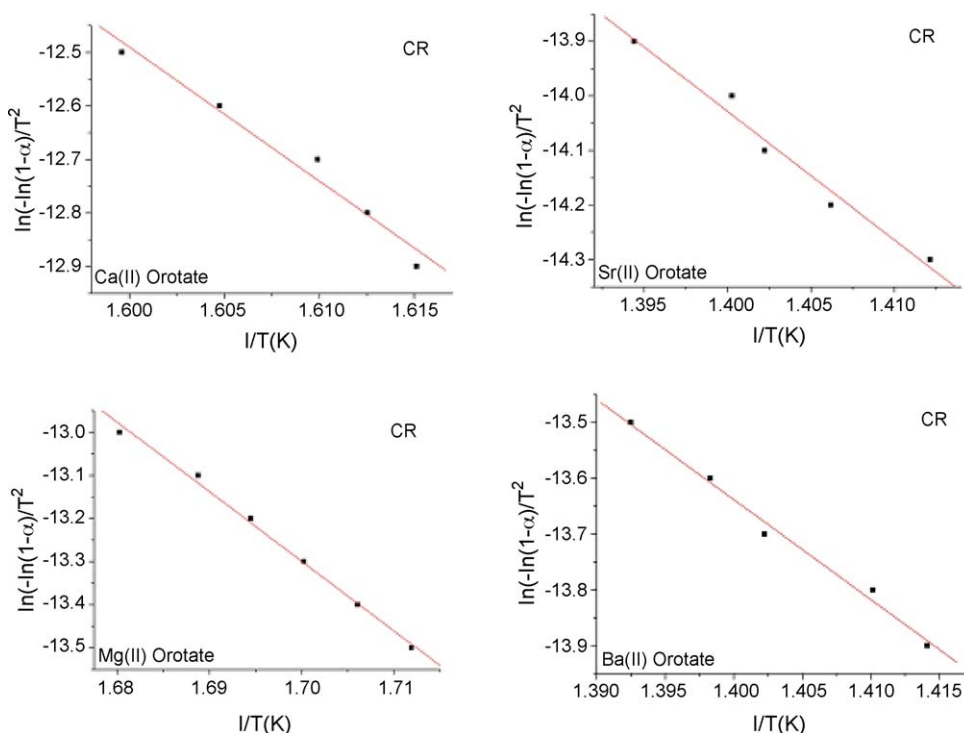


Fig. 6. Coats-Redfern(CR) of Ca(II), Mg(II), Ba(II) and Sr(II) orotate complexes.

Table 4

Thermodynamic data of the thermal decomposition Ca(II), Mg(II), Ba(II) and Sr(II) orotate complexes.

Complex	Parameter					<i>r</i>
	<i>E</i> (J mol <sup>-1</sup> )	<i>A</i> (s <sup>-1</sup> )	$\Delta S$ (J mol <sup>-1</sup> K <sup>-1</sup> )	$\Delta H$ (J mol <sup>-1</sup> )	$\Delta G$ (J mol <sup>-1</sup> )	
I	$2.08 \times 10^2$	$5.90 \times 10^{12}$	$-6.55 \times 10$	$-4.97 \times 10^3$	$-8.89 \times 10^2$	0.98522
II	$1.34 \times 10^2$	$5.51 \times 10^6$	$-1.22 \times 10^2$	$-4.76 \times 10^3$	$6.68 \times 10^4$	0.99741
III	$1.49 \times 10^2$	$4.38 \times 10^5$	$-1.44 \times 10^2$	$-5.79 \times 10^3$	$9.72 \times 10^4$	0.99489
IV	$1.96 \times 10^2$	$1.05 \times 10^9$	-79.5	$-5.74 \times 10^3$	$5.10 \times 10^4$	0.98761

Table 5

Antibacterial activity data of the ligands and their metal complexes, inhibition zone(mm).

Compound	<i>Bacillus subtilis</i> G <sup>+</sup>	<i>Staphylococcus aureus</i> G <sup>+</sup>	<i>Escherichia coli</i> G <sup>-</sup>	<i>Pseudomonas aeruginosa</i> G <sup>-</sup>
H <sub>2</sub> L	++	+	++	+
I	+++	++	++++	++
II	++	++	+++	++
III	+++	+++	++	++
IV	+++	-	+++	+

(-): NO antibacterial activity; (+): mild activity; (++) : moderate activity; (+++) : marked activity; (++++): strong marked activity.

results of the bactericidal screening of the synthesized compounds are recorded in Table 5. An influence of the central ion of the complexes in the antibacterial activity against the tested Gram positive and Gram negative organisms show that the complexes have an enhanced activity compared to the orotic acid itself.

## References

- [1] A.S. Akalin, S. Gone, Sci. Int. 51 (1996) 554.
- [2] P. Ruasmadiedo, J.C. Badagancedo, E.G. Fernandez, D.G. Dellano, C.G. Delos Reyes Gavilan, J. Food Protect. 59 (1996) 502.
- [3] O. Kumberger, J. Riedo, H. Smidbauer, Chem. Ber. 124 (1991) 2739.
- [4] N. Lalioti, C.P. Raptopoulou, A. Terzis, A. Panagiotopoulos, S.P. Perlepes, E. Manessi-Zoupa, J. Chem. Soc. Dalton Trans. 1327 (1998).
- [5] O. Kumberger, J. Riede, H. Schmidbauer, Z. Naturforsch. 48b (1993) 961.
- [6] H. Schmidbauer, H.G. Classen, J. Helbig, Angew. Chem., Int. Ed. Engl. 18 (1990) 1090.
- [7] K. Matsumoto, Inorg. Chim Acta 151 (1988) 9.
- [8] X. Li, R. Cao, D. Sun, Q. Shi, M. Hong, Y. Liang, Inorg. Chem. Commun. 5 (2002) 589.
- [9] M.J. Plater, M.R.S.J. Foreman, J.M.S. Skakle, R.A. Howie, Inorg. Chim. Acta 332 (2002) 135.
- [10] A.D. Burrows, C.W. Chan, M.M. Chowdhry, J.E. McGrady, D.M.P. Mingos, Chem. Soc. Rev. (1995) 329.
- [11] J. Victor, L.B. Greenberg, D.L. Sloan, J. Biol. Chem. 254 (1979) 2647.
- [12] H. Schmidbauer, H.G. Classen, J. Helbig, Angew. Chem. Int. Ed. Engl. 29 (1990) 1090.

- [13] K. Matsumoto, *Inorg. Chim. Acta* 151 (1988) 9.
- [14] Br.E. Doody, E.R. Tucci, R. Scruggs, N.C. Li, *J. Inorg. Nucl. Chem.* 28 (1996) 883.
- [15] F. Nepveu, N. Gaultier, N. Korber, J. Jaud, P. Castan, *J. Chem. Soc. Dalton Trans.* (1995) 4005.
- [16] G. Maistralis, A. Koutsodimou, N. Katsaros, *Transition Met. Chem.* 25 (2000) 166.
- [17] B.E. Doody, E.R. Tucci, R. Scruggs, N.C. Li, *J. Inorg. Nucl. Chem.* 28 (1966) 833.
- [18] A.K. Singh, R.P. Singh, *Indian J. Chem.* 17A (1979) 469.
- [19] M. Sabat, D. Zglinska, B. Jeznowska-Trzebiatowska, *Acta Crystallogr. B* 36 (1980) 1187.
- [20] A.Q. Wu, L.Z. Cai, G.H. Guo, F.K. Zheng, G.C. Guo, E.G. Mao, J.S. Huang, *Chin. J. Inorg. Chem.* 19 (2003) 879.
- [21] I. Mutikainen, R. Hamalainen, M. Klinga, O. Orama, U. Turpeinen, *Acta Crystallogr. C* 52 (1996) 2480.
- [22] H. Icbudak, H. Olmez, O.Z. Yesilel, F. Arslan, P. Naumov, G. Javanowski, A.R. Ibrahim, A. Umsan, H.K. Fun, S. Chantrapronma, S.W. Ng, *J. Mol. Struct.* 657 (2003) 225.
- [23] A. Karipides, B. Thomas, *Acta Crystallogr. C* 42 (1986) 1705.
- [24] V. Radecka-Paryzek, V. Patroniak, *Polyhedron* 13 (1994) 2125.
- [25] C.W. Bock, A.K. Katz, J.P. Glusker, *J. Am. Chem. Soc.* 117 (1995) 3754.
- [26] A.K. Katz, J.P. Glusker, S.A. Beele, C.W. Bock, *J. Am. Chem. Soc.* 118 (1996) 5732.
- [27] O. Karugo, K. Djinovic, M.J. Rizzi, *J. Chem. Soc. Dalton Trans.* (1993) 2127.
- [28] M. Peschke, A.T. Blades, P. Kebarle, *J. Phys. Chem. A* 102 (1998) 9978.
- [29] A. Karipides, B. Thomas, *Acta Crystallogr. C* 42 (1986) 1705.
- [30] I. Mutikainen, P. Lumme, *Acta Crystallogr. B* 36 (1980) 2233.
- [31] T. Solin, K. Matsumoto, K. Fuwa, *Bull. Chem. Soc. Jap.* 54 (1981) 3731.
- [32] T.S. Khodashova, M.A. Porai-Koshits, N.K. Davidenko, N.N. Vlasova, *Koord. Khim.* 10 (1984) 262.
- [33] L.S. Gelfand, F.J. Iaconianni, L.L. Pytlewski, A.N. Specca, C.M. Mikulski, N.M. Karayannis, *J. Inorg. Nucl. Chem.* 42 (1980) 377.
- [34] I. Mutikainen, P. Lumme, *Acta Crystallogr. B* 36 (1980) 2233.
- [35] S. Lencioni, A. Pellerito, T. Fiore, A.M. Giuliani, L. Pellerito, M.T. Cambria, C. Mansueto, *Appl. Organomet. Chem.* 31 (1999) 145.
- [36] A.W. Coats, J.P. Redfern, *Nature* 201 (1964) 68.